Radiotherapy and Oncology 175 (2022) 47–55

Contents lists available at ScienceDirect

Radiotherapy and Oncology

journal homepage: www.thegreenjournal.com

Original Article

A case-control study of linear energy transfer and relative biological effectiveness related to symptomatic brainstem toxicity following pediatric proton therapy

Lars Fredrik Fjæra [a,*], Daniel J. Indelicato [b], Andreas H. Handeland [a,c], Kristian S. Ytre-Hauge [a], Yasmin Lassen-Ramshad [d], Ludvig P. Muren [d,e], Camilla H. Stokkevåg [a,c]

[a] Department of Physics and Technology, University of Bergen, Bergen, Norway; [b] Department of Radiation Oncology, University of Florida, Jacksonville, Florida, USA; [c] Department of Oncology and Medical Physics, Haukeland University Hospital, Bergen, Norway; [d] Danish Centre for Particle Therapy, Aarhus University Hospital; and [e] Department of Clinical Medicine, Aarhus University, Aarhus, Denmark

ARTICLE INFO

Article history:
Received 7 April 2022
Received in revised form 28 June 2022
Accepted 25 July 2022
Available online 30 July 2022

Keywords:
Brainstem toxicity
Pediatrics
Proton therapy
Relative biological effectiveness (RBE)
Linear energy transfer (LET)

ABSTRACT

Background and purpose: A fixed relative biological effectiveness (RBE) of 1.1 ($RBE_{1.1}$) is used clinically in proton therapy even though the RBE varies with properties such as dose level and linear energy transfer (LET). We therefore investigated if symptomatic brainstem toxicity in pediatric brain tumor patients treated with proton therapy could be associated with a variable LET and RBE.

Materials and methods: 36 patients treated with passive scattering proton therapy were selected for a case-control study from a cohort of 954 pediatric brain tumor patients. Nine children with symptomatic brainstem toxicity were each matched to three controls based on age, diagnosis, adjuvant therapy, and brainstem $RBE_{1.1}$ dose characteristics. Differences across cases and controls related to the dose-averaged LET (LET_d) and variable RBE-weighted dose from two RBE models were analyzed in the high-dose region.

Results: LET_d metrics were marginally higher for cases vs. controls for the majority of dose levels and brainstem substructures. Considering areas with doses above 54 Gy($RBE_{1.1}$), we found a moderate trend of 13% higher median LET_d in the brainstem for cases compared to controls (P =.08), while the difference in the median variable RBE-weighted dose for the same structure was only 2% (P =.6).

Conclusion: Trends towards higher LET_d for cases compared to controls were noticeable across structures and LET_d metrics for this patient cohort. While case-control differences were minor, an association with the observed symptomatic brainstem toxicity cannot be ruled out.

Proton therapy offers a reduction in dose to normal tissues compared to conventional photon therapy. Since the majority of pediatric cancer patients are expected to become long-term survivors [1], children are often referred to proton therapy to minimize radiation damage. While the overall incidence of brainstem injury following cranial proton therapy is relatively low [2–4], it is a very serious side effect that can lead to symptoms such as ataxia, dysphagia, respiratory difficulty, and in worst case death [2].

Protons have a higher relative biological effectiveness (RBE) compared to photons. Clinically, the RBE is set to a constant value of 1.1, implying that protons are uniformly characterized as 10% more biologically effective than photons. The RBE of 1.1 ($RBE_{1.1}$) was determined as a conservative value mainly based on animal experiments conducted in the 1970s [5]. While a conservative RBE increases the probability of ensuring tumor control, an underestimation of the RBE may lead to overdosage of healthy tissue. It is also well known that the RBE is not constant but varies as a function of the linear energy transfer (LET). Considering that the LET increases rapidly at the distal dose fall-off of the proton beam, elevated RBE values are of particular concern for organs at risk located in vicinity of the fall-off. Moreover, the RBE has also been shown to increase for lower $(\alpha/\beta)_x$ ratios in the linear quadratic model as well as for lower dose levels [6]. While these effects have been quantified through both *in vitro* [5,7,8] and *in vivo* experiments [9,10], the clinical consequences are less clear. In recent years, several reports have emerged indicating a potential correlation between toxicity and increased RBE [11–19]. Nevertheless, the evidence for correlation is not decisive [20], in particular for symptomatic toxicity, emphasizing the need for further study.

* Corresponding author at: Department of Medical Physics, Oslo University Hospital, Norwegian Radium Hospital, P.O. Box 4953, Nydalen, NO-0424 Oslo, Norway.
E-mail address: larsff@ous-hf.no (L.F. Fjæra).

https://doi.org/10.1016/j.radonc.2022.07.022
0167-8140/

For pediatric brain tumor patients, the RBE variability in proton therapy may be particularly worrying for three reasons: (i) the brainstem is associated with low $(\alpha/\beta)_x$ ratios [21,22], (ii) fraction sizes are typically ≤2 Gy(RBE) [23], and (iii) the LET increases for smaller modulation widths of the spread-out Bragg peak [5] which is often the case when using smaller sized treatment fields commonly applied for children treated with proton therapy.

There is great emphasis on keeping brainstem doses below established constraints. Furthermore, to reduce RBE and range uncertainties associated with proton beams, a common approach is to minimize the number of treatment fields ranging out within the brainstem [2,4,6]. There are, however, still persistent concerns about brainstem toxicity following cranial proton therapy, and regional differences in radiosensitivity of this vital brain structure have been indicated which might influence the incidence of toxicity [21,24,25]. The purpose of this study was therefore to investigate if symptomatic brainstem toxicity in pediatric brain tumor patients treated with proton therapy can be associated with a varying LET and RBE, and whether this effect is specific to anatomic subsites within the brainstem.

Materials and methods

Patient material

An anonymized cohort selected from 954 pediatric patients with brain tumors treated with double scattering proton therapy at the University of Florida Health Proton Therapy Institute (UFHPTI) between 2006 and 2017 were used in this institutional review board-approved case-control study. Symptomatic brainstem toxicity was defined as new or progressive symptoms not attributable to tumor progression, and further characterized as grade 2+ response according to the Common Terminology Criteria for Adverse Events (CTCAE) version 4.0. Overall, 16 cases of the 954 patients experienced symptomatic brainstem toxicity. Seven cases were excluded either due the lack of appropriate controls in the high dose region or due to intrinsic compromise of brainstem integrity. Each of the nine resulting cases was closely matched to three separate controls based on age (±1.5 years), diagnosis, adjuvant therapy, and brainstem $RBE_{1.1}$ dose parameters ($D_{10\%}$ ± 2 Gy (RBE), $D_{0.1cc}$ ± 2 Gy(RBE)). All patients had clinical target volumes (CTVs) defined in addition to planning target volumes (PTVs) (CTV plus a 3 mm isotropic margin). The brainstem, including the brainstem core (brainstem cropped by 3 mm) and brainstem surface (3 mm edge of the brainstem), were delineated for treatment planning. For the purpose of this study, T1/T2 weighted magnetic resonance imaging (MRI) scans fused with computed tomography (CT) scans were used to define the substructures of the brainstem which included the midbrain, pons, and medulla oblongata (Fig. 1).

The patients had been diagnosed with either craniopharyngioma or ependymoma. The standard prescription doses ranged between 54.0 and 59.4 Gy(RBE), delivered in fractions of 1.8 Gy (RBE). An example of a dose distribution is shown in Fig. 1. The planning objectives were based on UFHPTI clinical protocols, where the CTV should be encompassed by the 99% isodose line and the PTV should be encompassed by the 95% isodose line of the prescribed dose. Clinically approved dosimetric constraints to the brainstem and organs at risk [2,4] were used during treatment planning in the Eclipse (Varian Medical Systems, Palo Alto, CA) treatment planning system (TPS).

Monte Carlo simulations

To obtain LET and variable RBE-weighted doses, the CT images as well as treatment plan information for the 36 patients were imported into the FLUKA Monte Carlo (MC) code [26–28] version 2011.2x. We have previously developed a framework that allows for recalculation of proton plans in FLUKA. This framework includes translation of treatment plan information and semi-automatic setup of the recalculation system, as well as methods to obtain LET [29] and variable RBE-weighted doses from multiple RBE models [30]. To allow for an accurate recalculation of the proton therapy plans, a detailed model of the double scattering treatment nozzle at the UFHPTI was implemented and commissioned in an earlier publication [31].

The number of treatment fields for each proton plan ranged between two and five. Each field was simulated separately with 600 million primary protons, and scoring files were combined during post-processing. We scored the physical dose, dose-averaged LET (LET_d), as well as the LET spectra on a voxel-by-voxel basis using the same scoring grid specifications as in the clinical treatment plans. Using proton stopping power ratios, the dose and LET were converted to dose-to-water and LET-to-water,

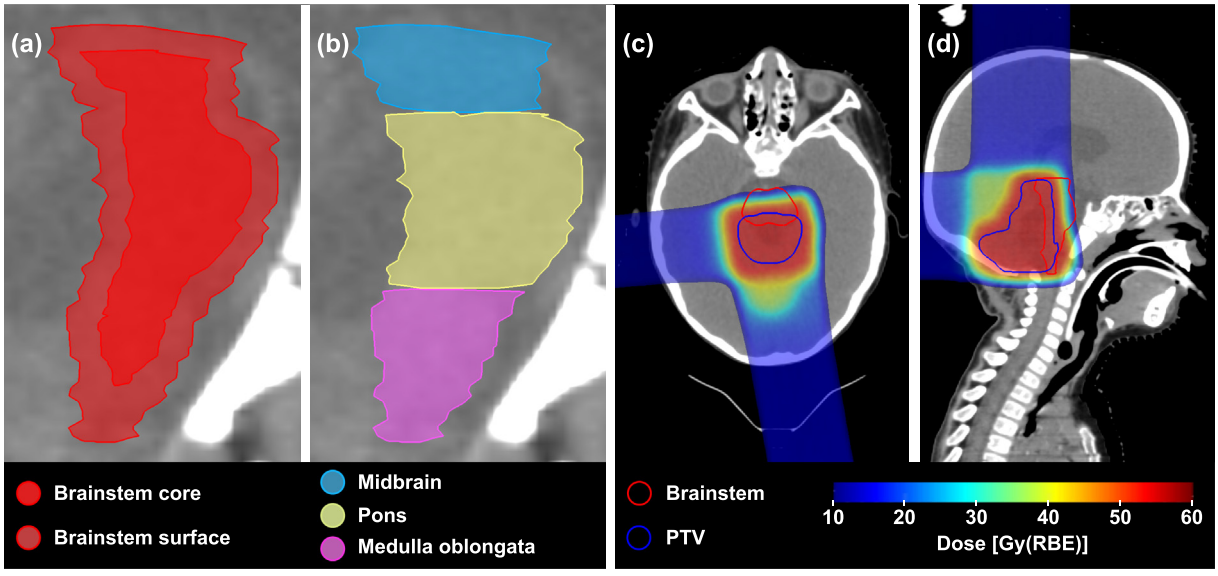

Fig. 1. (a-b) Substructures of the brainstem projected onto a cropped CT image. (c-d) $RBE_{1.1}$-weighted dose distribution for a patient.

respectively (details found in [31]). The dose was calculated taking all particles into consideration, while the LET calculations were based on primary and secondary protons only. To maintain consistency with the clinically calculated TPS dose, and not focus on differences in dose calculation algorithms, the MC recalculated physical dose distributions were in post-processing normalized to the median CTV dose that was obtained during the initial treatment planning, with normalization factors ranging between −3.2% and 2.4%. The normalized dose distributions were used in the analysis of both $RBE_{1.1}$ and variable RBE-weighted doses, while the reported LET values were unaffected by the normalization.

RBE models

To account for biological variation in the treated patients we obtained variable RBE-weighted doses using the non-linear phenomenological model by Rørvik et al. (ROR) [32] which requires the full LET spectrum to estimate the RBE. Phenomenological models have a tissue dependency quantified by the $(\alpha/\beta)_x$ in the linear quadratic model. An $(\alpha/\beta)_x$ of 2.1 Gy [21,22] was used for the brainstem and brainstem substructures. Since phenomenological RBE models and $(\alpha/\beta)_x$ ratios are associated with considerable uncertainties, we also included the simpler LET-weighted dose (LWD) where the $RBE = 1 + c \cdot LET_d$. The c parameter is a scaling factor used to quantify the biological response. It was set to 0.055 μm/keV, a value based on fits to *in vitro* data in order to minimize the biological variability, i.e., the range of biological response for a given dose [33].

Data analysis and statistics

RBE-weighted doses from $RBE_{1.1}$, as well as ROR and the LWD were evaluated using volume histograms with dose and LET_d metrics at the median volume ($D_{50\%}/L_{50\%}$), 10% volume ($D_{10\%}/L_{10\%}$) and 0.1 cc ($D_{0.1cc}/L_{0.1cc}$) in the brainstem as a primary analysis to investigate potential trends between cases and controls. Furthermore, we also considered brainstem substructures to investigate possible regional differences in the dosimetric parameters. High LET_d alone does not necessarily translate to a high biological effect since biological damage is also greatly dependent on the dose level. In order to assess LET_d metrics independently, but also in the context of biological damage, we applied multiple dose cutoff values for the LET_d evaluation. Hence, the LET_d values were overwritten and set to zero in voxels receiving doses below the applied cutoff. However, this has consequences when calculating metrics based on relative volumes as artificially set zero-values in structures will shift metrics towards zero. Thus, LET_d metrics for relative volumes such as $L_{50\%}$ and $L_{10\%}$ were calculated only for the subvolume of the structure receiving dose above the cutoff. The cutoffs applied were 1, 20, 40, 50, 54 and 55 Gy(RBE) based on the $RBE_{1.1}$ dose.

Conditional logistic regression, appropriate for case-control groups matched on several criteria, was used to detect statistically significant differences between metrics for cases and controls. An advantage of conditional logistic regression over regular logistic regression is its ability to minimize the confounding introduced from the matching criteria [34]. Univariate conditional logistic regression models were fitted to the dose and LET_d metrics outlined by minimizing the negative log-likelihood of the function with respect to the data points. P values were obtained by the two-tailed area excluded by the normal distribution based on the parameter associated with the given factor and the calculated standard error. The conditional logistic regression was done using the conditional logit function from the *Statsmodels* Python package [35]. The 95% confidence intervals (95% CIs) for cases and controls were also obtained using a basic t-test from the standard error of cases and controls, adjusted for sample size, with overlapping CIs between cases and controls also giving an indication of the statistical significance of the results.

Results

In areas receiving doses of 54 Gy(RBE) or higher, the median LET_d, $L_{10\%}$, and $L_{0.1cc}$ showed trends towards higher average values for the symptomatic brainstem necrosis cases compared to the controls in the brainstem (Fig. 2), with cases having an average median LET_d of 2.7 keV/μm (95% CI: 2.5–2.9 keV/μm) compared to controls with an average value of 2.4 keV/μm (95% CI: 2.2–2.6 keV/μm) (P =.08). The trends became more obvious when smaller volumes were considered with differences in case-control means for $L_{10\%}$ at 3.1 keV/μm (95% CI: 2.8–3.5 keV/μm) vs. 2.8 keV/μm (95% CI: 2.7–2.9) (P =.05) and $L_{0.1cc}$ at 3.4 keV/μm (95% CI: 2.9–3.8 keV/μm) vs. 3.0 keV/μm (95% CI: 2.9–3.2 keV/μm) (P =.06). The trend towards higher metrics for cases compared to controls was less evident when applying a dose cutoff of only 1 Gy(RBE), where in the case of the median LET_d in the brainstem an average of 3.3 keV/μm (95% CI: 2.8–3.8 keV/μm) was found for cases and 3.1 keV/μm (95% CI: 2.8–3.3 keV/μm) for controls (P =.3). Similar slightly increased average values for cases compared to controls were also observed for the majority of brainstem substructures (Fig. 2) and explored dose cutoffs (Supplementary Materials Fig. S1), but with very few differences showing statistical significance with P values below 0.05 (Supplementary Materials Tables S1–S3). LET_d volume histograms for the brainstem did not reveal any obvious trends regarding case-control differences (Fig. 3). This was also evident for the brainstem substructures.

LET_d distributions, at a 50 Gy(RBE) dose threshold, for all cases and controls along with corresponding median LET_d and RBE-weighted doses in the brainstem are shown in Fig. 4. LET_d hotspots were clearly visible for the majority of both cases and controls, frequently located either within the brainstem, or ventral or caudal to the brainstem.

The median $RBE_{1.1}$ dose for the cases trended towards marginally higher averages compared to the controls for the brainstem with an increasing case-control dose difference when using ROR or LWD to estimate the variable RBE-weighted dose (Fig. 5 and Supplementary Materials Table S4). Such trends were also evident when comparing cases and controls in each group individually, as well as for $D_{10\%}$ and $D_{0.1cc}$ but with negligible differences in absolute values since these metrics were part of the matching criteria (Supplementary Materials Figs. S2–S3 and Tables S5–S6). For the brainstem substructures the average differences between cases and controls in median dose using $RBE_{1.1}$, ROR and LWD fluctuated around zero (Fig. 5 and Supplemetary Materials Table S4), while differences in $D_{10\%}$ and $D_{0.1cc}$ were negligible (Supplementary Materials Figs. S2–S3 and Tables S5-S6).

In all but three case-control groups, at least one control received higher maximum ROR dose to the brainstem compared to the case, not revealing any systematic case-control differences (Supplementary Materials Fig. S4). This was also similar for the brainstem substructures as well as for the LWD.

Discussion

In this case-control study we investigated the impact of variable RBE-weighted doses and LET_d on brainstem toxicity for 36 pediatric patients treated with proton therapy. The case-control differences were generally small for both RBE-weighted dose and LET_d, with high heterogeneity, wide confidence intervals and insignificant P values. Nevertheless, the average case typically trended towards higher LET_d to the brainstem for similar doses, as well as for most brainstem substructures. There was also a minor trend

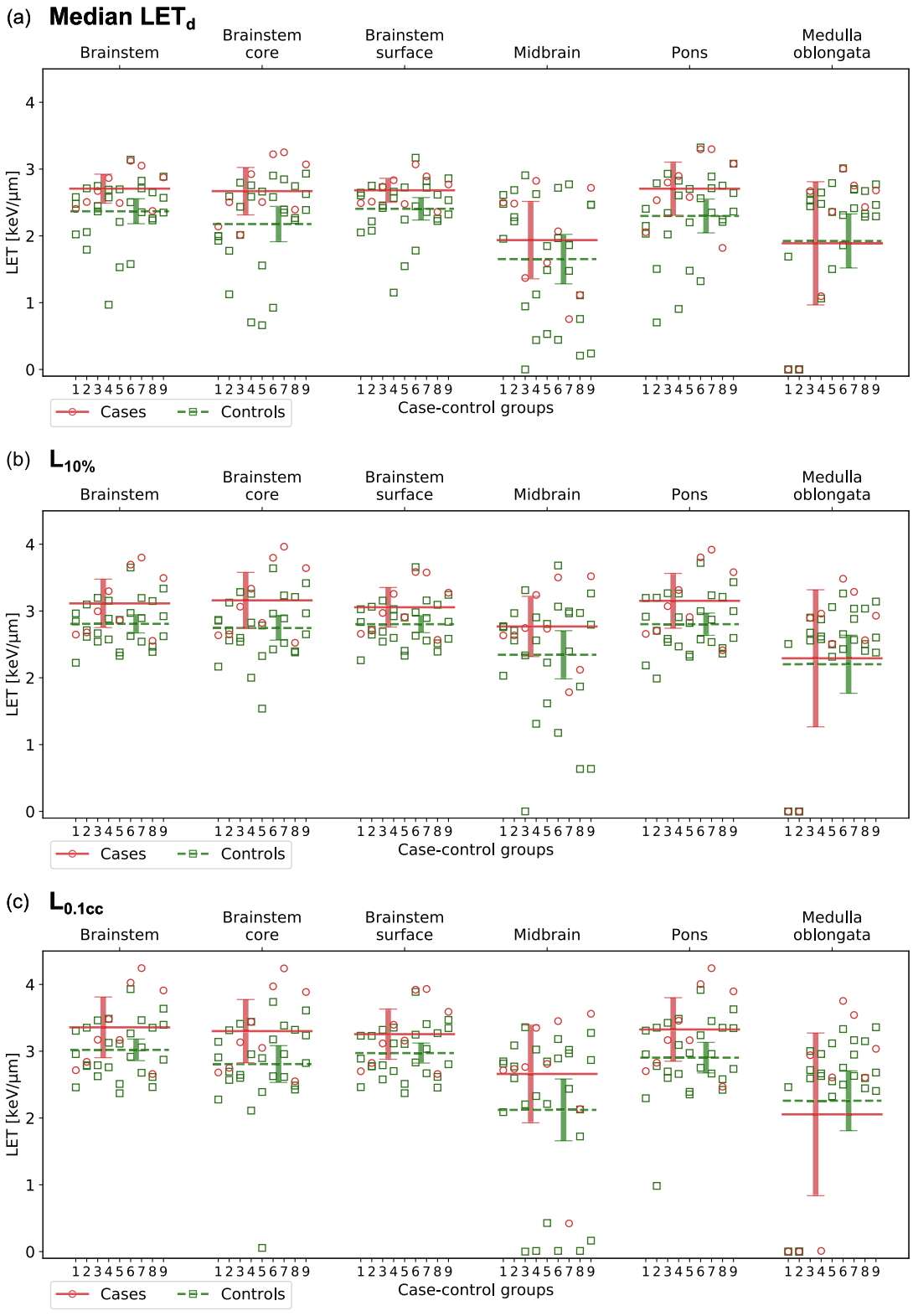

Fig. 2. Median LET_d (a), LET_d at 10% volume ($L_{10\%}$) (b), and LET_d at 0.1 cc volume ($L_{0.1cc}$) (c) with a 54 Gy(RBE) dose cutoff for cases (red circles) and controls (green squares) in the brainstem and brainstem substructures. Horizontal lines show average values for cases (red solid lines) and controls (green dashed lines), while vertical error bars depict 95% confidence intervals. (For interpretation of the references to color in this figure, the reader is referred to the web version of this article).

towards increased RBE-weighted dose differences between cases and controls when comparing variable RBE models to $RBE_{1.1}$ doses.

Multiple published studies have found a correlation between image changes, i.e., CTCAE grade 1 toxicity and LET/RBE [11,14,16–19], while others have been unable to identify a significant correlation [36–38]. While the degree to which image changes clinically impact patients is unclear [39], a potential advantage of including patients with asymptomatic toxicity is that such patients

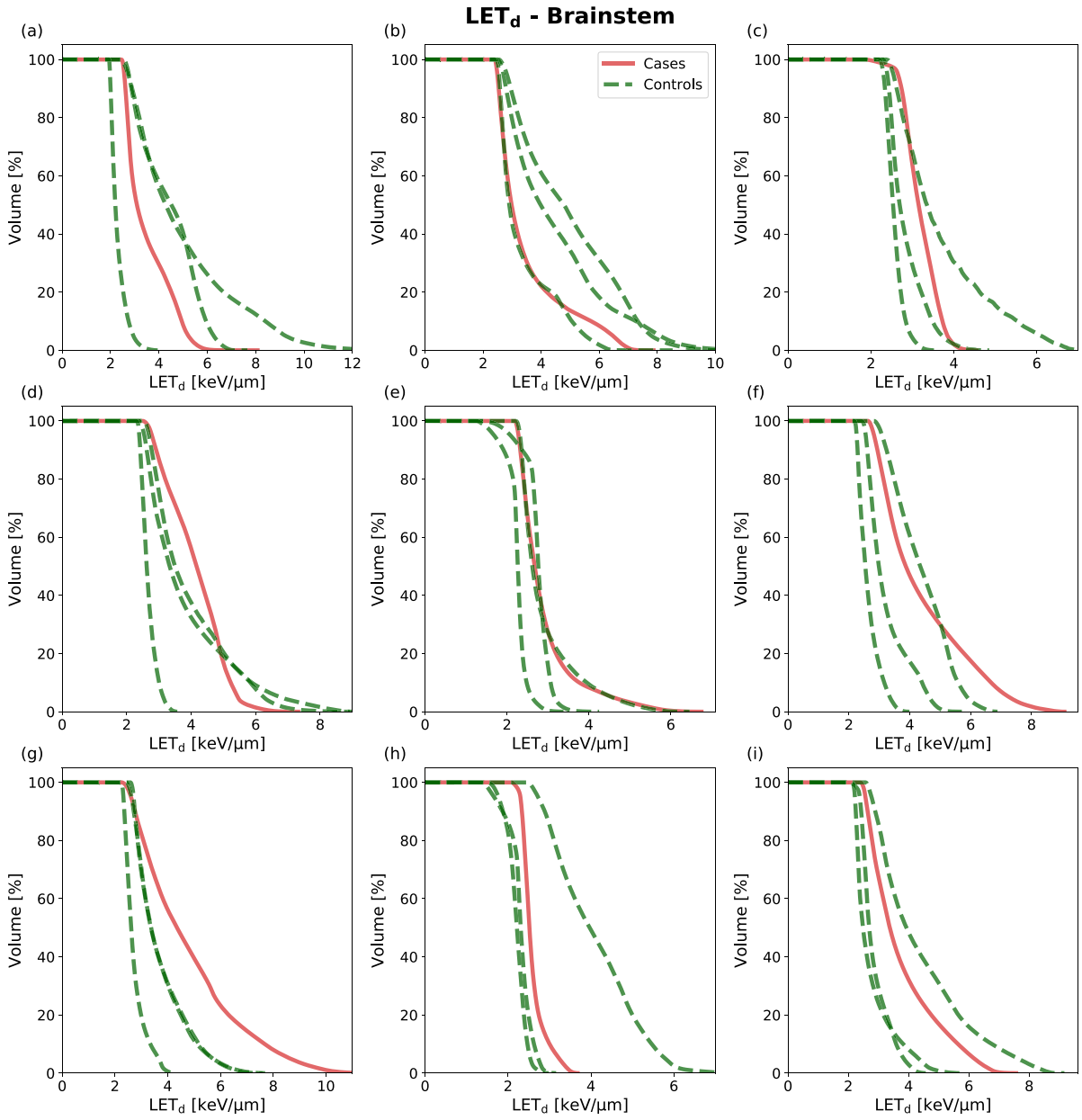

Fig. 3. LET$_d$ volume histograms for the brainstem for each matched group with cases (red solid lines) and controls (green dashed lines). No dose cutoff has been applied. The x-axes vary between different patient groups. (For interpretation of the references to color in this figure, the reader is referred to the web version of this article).

are more abundant compared to individuals diagnosed with symptomatic toxicity. For example, the incidence of symptomatic brainstem toxicity for pediatric brain tumor patients following proton have been reported to be approximately 2% [4]. While the low incidence is fortunate, the serious nature of these side effects calls for investigation. Nevertheless, clinically applied efforts to reduce LET in vital organs [2,4,6] coupled with the low incidence of symptomatic brainstem necrosis as well as the difficulty of distinguishing between symptomatic toxicity and disease progression [22], complicates the task of acquiring a sufficient amount of patients to draw definitive conclusions regarding the clinical effects of the RBE variability [40], particularly for this clinical endpoint. For instance, in a recently published study, a power analysis was conducted for head and neck cancer patients treated with intensity-modulated proton therapy. The authors estimated that a data set consisting of over 15,000 patients would be required to determine a definitive correlation between a variable RBE and toxicity for this patient group [41]. Nonetheless, the trends observed in this study coupled with previous evidence should warrant further investigation and clinical precautions with regard to LET.

Several dose cutoffs for the LET$_d$ were applied in order to explore the isolated clinical effect of the LET, while maintaining the context of biological damage which requires a certain dose level. As a result, metrics based on relative volumes for the LET$_d$ were only calculated for voxels with doses above the applied cutoff, and not for the full structure. It should therefore be kept in mind that the reported LET$_d$ metrics at 50% (median) and 10% volumes are only considering the subvolume of voxels above the dose cutoff, hence leading to decreased absolute volumes. A consequence was therefore a higher $L_{50\%}$ and/or $L_{10\%}$ compared to $L_{0.1cc}$ for certain high dose cutoffs (Fig. 2 and Supplementary Fig. S1), due to the relative volumes reaching below an absolute value of

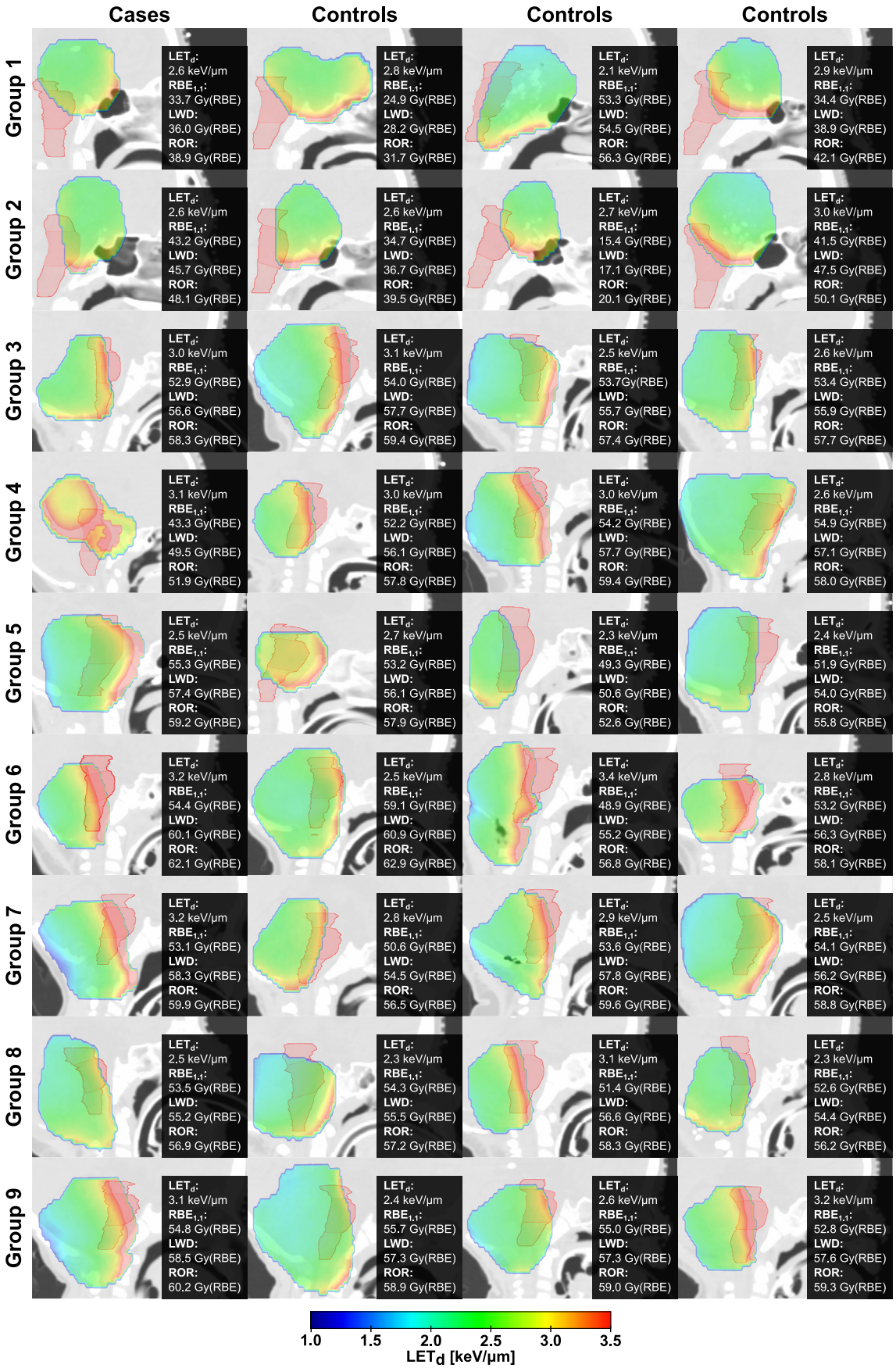

Fig. 4. LET$_d$ distributions for all patients in voxels with RBE$_{1.1}$ doses of 50 Gy(RBE) or above. Boxes in the bottom right corners list median LET$_d$, as well as median doses from RBE$_{1.1}$, ROR, and LWD in the brainstem. Midbrain, pons, and medulla oblongata (from top to bottom) are delineated in red. The sagittal plane is centred in the pons and cropped window sizes have been normalized for all patients.

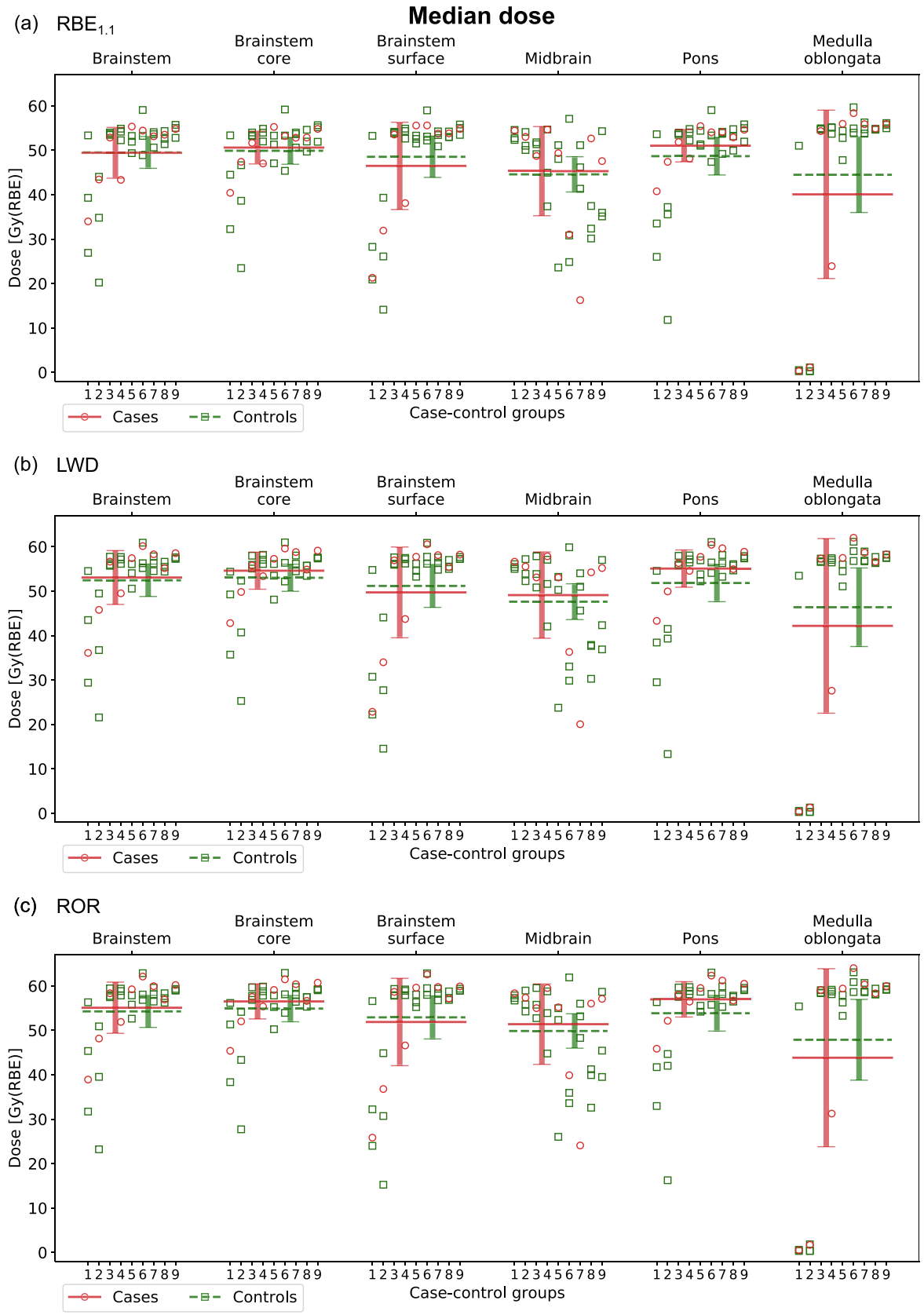

Fig. 5. Median doses from $RBE_{1.1}$ (a), LWD (b) and ROR (c) for cases (red circles) and controls (green squares) in the brainstem and brainstem substructures. Horizontal lines show average values for cases (red solid lines) and controls (green dashed lines), while vertical error bars depict 95% confidence intervals. (For interpretation of the references to color in this figure, the reader is referred to the web version of this article).

0.1 cc. Nevertheless, the trend of higher average LET_d metrics for cases vs. controls was generally consistent regardless of the applied dose cutoff, evaluated metric or structure. It is also important to note that the LET_d was scored using only primary and secondary protons, in agreement with the majority of previously published papers on LET_d in proton therapy [42]. Including heavier particles would increase the calculated LET_d [43,44], in particular in the entrance region of the proton beam [45]. Nevertheless, until there is a consensus in the scientific community regarding which particles to include for LET_d calculation or which LET-averaging method to use [46], the most important measure is to precisely report the method of LET calculation [42].

The substructures were separately evaluated in order to identify any trends in LET_d or RBE-weighted dose to specific sections of the brainstem. While there was a certain variance in both LET_d and RBE-weighted dose to the substructures, no obvious trends were identified, with the uncertainty in the origin of the brainstem necrosis also contributing towards the inconclusiveness of the substructure analysis. As the necrosis for a case should hypothetically originate from a single substructure, regarding all patients with symptomatic brainstem toxicity as cases for all substructures could introduce ambiguity. This could have been resolved if the precise location of the origin of the necrosis were known with certainty.

In our study, suitable follow-up MRI images were not available, therefore only dosimetric trends related to symptomatic brainstem toxicity as an endpoint could have been discovered through this analysis. Identifying regional differences in radiosensitivity within the brainstem could have been merged with such follow-up MRI images and potential image changes related to toxicity could have been analyzed in relation to the specific substructures. It should, however, be emphasized that image changes are associated with significant uncertainties, especially regarding the origin of necrosis [19,38]. Hence, a study of grade 2+ brainstem necrosis focuses more on the general organ volume of the patient where a voxel-wise analysis of image changes (grade 1) might take away from this focus on symptomatic disease, which additionally is of increased clinical relevance due to their severity and potential lethality compared to the asymptomatic nature of image changes. Furthermore, all structures were evaluated based on the same $(\alpha/\beta)_x$ value of 2.1. If a significant regional difference in radiosensitivity within the brainstem exists, it would have to be reflected through different $(\alpha/\beta)_x$ values for each substructure, which further would have affected the doses calculated by the phenomenological ROR model.

In conclusion, we identified very minor trends towards increased RBE-weighted dose to cases compared to controls. Case-control trends were more apparent when considering LET_d as the average case received higher LET_d than the average control for nearly all dose levels and brainstem substructures. There was, however, a substantial interpatient variability leading to wide confidence intervals and case-control differences that generally could not be considered statistically significant. Nevertheless, due to trends observed in this study we believe that individual assessment of LET in clinics should be explored further and successful application may provide safer delivery of proton therapy for patients at risk of brainstem toxicity.

Conflict of interest

The authors report no conflicts of interest.

Acknowledgements

This work was partly funded by the Trond Mohn Foundation (funding no. BFS2015TMT03) and The Norwegian Cancer Society (202089).

Appendix A. Supplementary material

Supplementary data to this article can be found online at https://doi.org/10.1016/j.radonc.2022.07.022.

References

[1] Oeffinger KC, Mertens AC, Sklar CA, Kawashima T, Hudson MM, Meadows AT, et al. Chronic health conditions in adult survivors of childhood cancer. N Engl J Med 2006;355:1572–82. https://doi.org/10.1056/NEJMsa060185.
[2] Indelicato DJ, Flampouri S, Rotondo RL, Bradley JA, Morris CG, Aldana PR, et al. Incidence and dosimetric parameters of pediatric brainstem toxicity following proton therapy. Acta Oncol 2014;53:1298–304. https://doi.org/10.3109/0284186X.2014.957414.
[3] Gentile MS, Yeap BY, Paganetti H, Goebel CP, Gaudet DE, Gallotto SL, et al. Brainstem injury in pediatric patients with posterior fossa tumors treated with proton beam therapy and associated dosimetric factors. Int J Radiat Oncol Biol Phys 2018;100:719–29. https://doi.org/10.1016/j.ijrobp.2017.11.026.
[4] Haas-Kogan D, Indelicato D, Paganetti H, Esiashvili N, Mahajan A, Yock T, et al. National cancer institute workshop on proton therapy for children: considerations regarding brainstem injury. Int J Radiat Oncol Biol Phys 2018;101:152–68. https://doi.org/10.1016/j.ijrobp.2018.01.013.
[5] Paganetti H. Relative biological effectiveness (RBE) values for proton beam therapy. Variations as a function of biological endpoint, dose, and linear energy transfer. Phys Med Biol 2014;59:R419–72. https://doi.org/10.1088/0031-9155/59/22/R419.
[6] Paganetti H, Blakely E, Carabe-Fernandez A, Carlson DJ, Das IJ, Dong L, et al. Report of the AAPM TG-256 on the relative biological effectiveness of proton beams in radiation therapy. Med Phys 2019;46:e53–78. https://doi.org/10.1002/mp.13390.
[7] Mara E, Clausen M, Khachonkham S, Deycmar S, Pessy C, Dorr W, et al. Investigating the impact of alpha/beta and LETd on relative biological effectiveness in scanned proton beams: an in vitro study based on human cell lines. Med Phys 2020;47:3691–702. https://doi.org/10.1002/mp.14212.
[8] Sørensen BS, Overgaard J, Bassler N. In vitro RBE-LET dependence for multiple particle types. Acta Oncol 2011;50:757–62. https://doi.org/10.3109/0284186X.2011.582518.
[9] Sørensen BS, Bassler N, Nielsen S, Horsman MR, Grzanka L, Spejlborg H, et al. Relative biological effectiveness (RBE) and distal edge effects of proton radiation on early damage in vivo. Acta Oncol 2017;56:1387–91. https://doi.org/10.1080/0284186X.2017.1351621.
[10] Saager M, Peschke P, Brons S, Debus J, Karger CP. Determination of the proton RBE in the rat spinal cord: Is there an increase towards the end of the spread-out Bragg peak? Radiother Oncol 2018;128:115–20. https://doi.org/10.1016/j.radonc.2018.03.002.
[11] Peeler CR, Mirkovic D, Titt U, Blanchard P, Gunther JR, Mahajan A, et al. Clinical evidence of variable proton biological effectiveness in pediatric patients treated for ependymoma. Radiother Oncol 2016;121:395–401. https://doi.org/10.1016/j.radonc.2016.11.001.
[12] Wang CC, McNamara AL, Shin J, Schuemann J, Grassberger C, Taghian AG, et al. End-of-range radiobiological effect on rib fractures in patients receiving proton therapy for breast cancer. Int J Radiat Oncol Biol Phys 2020;107:449–54. https://doi.org/10.1016/j.ijrobp.2020.03.012.
[13] Bertolet A, Abolfath R, Carlson DJ, Lustig RA, Hill-Kayser C, Alonso-Basanta M, et al. Correlation of LET with MRI changes in brain and potential implications for normal tissue complication probability for patients with meningioma treated with pencil beam scanning proton therapy. Int J Radiat Oncol Biol Phys 2022;112:237–46. https://doi.org/10.1016/j.ijrobp.2021.08.027.
[14] Ödén J, Toma-Dasu I, Witt Nystrøm P, Traneus E, Dasu A. Spatial correlation of linear energy transfer and relative biological effectiveness with suspected treatment-related toxicities following proton therapy for intracranial tumors. Med Phys 2020;47:342–51. https://doi.org/10.1002/mp.13911.
[15] Underwood TSA, Grassberger C, Bass R, MacDonald SM, Meyersohn NM, Yeap BY, et al. Asymptomatic late-phase radiographic changes among chest-wall patients are associated with a proton RBE exceeding 1.1. Int J Radiat Oncol Biol Phys 2018;101:809–19. https://doi.org/10.1016/j.ijrobp.2018.03.037.
[16] Eulitz J, Troost EGC, Raschke F, Schulz E, Lutz B, Dutz A, et al. Predicting late magnetic resonance image changes in glioma patients after proton therapy. Acta Oncol 2019;58:1536–9. https://doi.org/10.1080/0284186X.2019.1631477.
[17] Bahn E, Bauer J, Harrabi S, Herfarth K, Debus J, Alber M. Late contrast enhancing brain lesions in proton-treated patients with low-grade glioma: clinical evidence for increased periventricular sensitivity and variable RBE. Int J Radiat Oncol Biol Phys 2020;107:571–8. https://doi.org/10.1016/j.ijrobp.2020.03.013.
[18] Bolsi A, Placidi L, Pica A, Ahlhelm FJ, Walser M, Lomax AJ, et al. Pencil beam scanning proton therapy for the treatment of craniopharyngioma complicated with radiation-induced cerebral vasculopathies: a dosimetric and linear energy transfer (LET) evaluation. Radiother Oncol 2020;149:197–204. https://doi.org/10.1016/j.radonc.2020.04.052.
[19] Engeseth GM, He R, Mirkovic D, Yepes P, Mohamed ASR, Stieb S, et al. Mixed effect modeling of dose and linear energy transfer correlations with brain image changes after intensity modulated proton therapy for skull base head and neck cancer. Int J Radiat Oncol Biol Phys 2021;111:684–92. https://doi.org/10.1016/j.ijrobp.2021.06.016.

[20] Paganetti H. Mechanisms and review of clinical evidence of variations in relative biological effectiveness in proton therapy. Int J Radiat Oncol Biol Phys 2022;112:222–36. https://doi.org/10.1016/j.ijrobp.2021.08.015.
[21] Meeks SL, Buatti JM, Foote KD, Friedman WA, Bova FJ. Calculation of cranial nerve complication probability for acoustic neuroma radiosurgery. Int J Radiat Oncol Biol Phys 2000;47:597–602. https://doi.org/10.1016/s0360-3016(00)00493-4.
[22] Mayo C, Yorke E, Merchant TE. Radiation associated brainstem injury. Int J Radiat Oncol Biol Phys 2010;76:S36–41. https://doi.org/10.1016/j.ijrobp.2009.08.078.
[23] Bates JE, Indelicato DJ, Morris CG, Rotondo RL, Bradley JA. Visual decline in pediatric survivors of brain tumors following radiotherapy. Acta Oncol 2020;59:1257–62. https://doi.org/10.1080/0284186X.2020.1803500.
[24] Hua C, Merchant TE, Gajjar A, Broniscer A, Zhang Y, Li Y, et al. Brain tumor therapy-induced changes in normal-appearing brainstem measured with longitudinal diffusion tensor imaging. Int J Radiat Oncol Biol Phys 2012;82:2047–54. https://doi.org/10.1016/j.ijrobp.2011.03.057.
[25] Uh J, Merchant TE, Li Y, Feng T, Gajjar A, Ogg RJ, et al. Differences in brainstem fiber tract response to radiation: a longitudinal diffusion tensor imaging study. Int J Radiat Oncol Biol Phys 2013;86:292–7. https://doi.org/10.1016/j.ijrobp.2013.01.028.
[26] Ferrari A, Sala PR, Fassó A, Ranft J. FLUKA: A multi-particle transport code. CERN-2005-10, INFN/TC_05/11, SLAC-R-773; 2005. https://www.slac.stanford.edu/pubs/slacreports/reports16/slac-r-773.pdf.
[27] Böhlen TT, Cerutti F, Chin MPW, Fassò A, Ferrari A, Ortega PG, et al. The FLUKA code: developments and challenges for high energy and medical applications. Nucl Data Sheets 2014;120:211–4. https://doi.org/10.1016/j.nds.2014.07.049.
[28] Battistoni G, Bauer J, Boehlen TT, Cerutti F, Chin MP, Dos Santos AR, et al. The FLUKA code: an accurate simulation tool for particle therapy. Front Oncol 2016;6:116. https://doi.org/10.3389/fonc.2016.00116.
[29] Fjæra LF, Li Z, Ytre-Hauge KS, Muren LP, Indelicato DJ, Lassen-Ramshad Y, et al. Linear energy transfer distributions in the brainstem depending on tumour location in intensity-modulated proton therapy of paediatric cancer. Acta Oncol 2017;56:763–8. https://doi.org/10.1080/0284186X.2017.1314007.
[30] Rørvik E, Fjæra LF, Dahle TJ, Dale JE, Engeseth GM, Stokkevåg CH, et al. Exploration and application of phenomenological RBE models for proton therapy. Phys Med Biol 2018;63:185013. https://doi.org/10.1088/1361-6560/aad9db.
[31] Fjæra LF, Indelicato DJ, Stokkevåg CH, Muren LP, Hsi WC, Ytre-Hauge KS. Implementation of a double scattering nozzle for Monte Carlo recalculation of proton plans with variable relative biological effectiveness. Phys Med Biol 2020;65. https://doi.org/10.1088/1361-6560/abc12d.
[32] Rørvik E, Thörnqvist S, Stokkevåg CH, Dahle TJ, Fjæra LF, Ytre-Hauge KS. A phenomenological biological dose model for proton therapy based on linear energy transfer spectra. Med Phys 2017;44:2586–94. https://doi.org/10.1002/mp.12216.
[33] McMahon SJ, Paganetti H, Prise KM. LET-weighted doses effectively reduce biological variability in proton radiotherapy planning. Phys Med Biol 2018;63:225009. https://doi.org/10.1088/1361-6560/aae8a5.
[34] Pearce N. Analysis of matched case-control studies. BMJ 2016;352:i969. https://doi.org/10.1136/bmj.i969.
[35] Seabold S, Perktold J. Statsmodels: Econometric and Statistical Modeling with Python. In: 9th Python in Science. https://doi.org/10.25080/majora-92bf1922-011.
[36] Giantsoudi D, Sethi RV, Yeap BY, Eaton BR, Ebb DH, Caruso PA, et al. Incidence of CNS injury for a cohort of 111 patients treated with proton therapy for medulloblastoma: LET and RBE associations for areas of injury. Int J Radiat Oncol Biol Phys 2016;95:287–96. https://doi.org/10.1016/j.ijrobp.2015.09.015.
[37] Garbacz M, Cordoni FG, Durante M, Gajewski J, Kisielewicz K, Krah N, et al. Study of relationship between dose, LET and the risk of brain necrosis after proton therapy for skull base tumors. Radiother Oncol 2021;163:143–9. https://doi.org/10.1016/j.radonc.2021.08.015.
[38] Niemierko A, Schuemann J, Niyazi M, Giantsoudi D, Maquilan G, Shih HA, et al. Brain necrosis in adult patients after proton therapy: is there evidence for dependency on linear energy transfer? Int J Radiat Oncol Biol Phys 2021;109:109–19. https://doi.org/10.1016/j.ijrobp.2020.08.058.
[39] Gunther JR, Sato M, Chintagumpala M, Ketonen L, Jones JY, Allen PK, et al. Imaging changes in pediatric intracranial ependymoma patients treated with proton beam radiation therapy compared to intensity modulated radiation therapy. Int J Radiat Oncol Biol Phys 2015;93:54–63. https://doi.org/10.1016/j.ijrobp.2015.05.018.
[40] Sørensen BS, Pawelke J, Bauer J, Burnet NG, Dasu A, Høyer M, et al. Does the uncertainty in relative biological effectiveness affect patient treatment in proton therapy? Radiother Oncol 2021;163:177–84. https://doi.org/10.1016/j.radonc.2021.08.016.
[41] Wagenaar D, Schuit E, van der Schaaf A, Langendijk JA, Both S. Can the mean linear energy transfer of organs be directly related to patient toxicities for current head and neck cancer intensity-modulated proton therapy practice? Radiother Oncol 2021;165:159–65. https://doi.org/10.1016/j.radonc.2021.09.003.
[42] Kalholm F, Grzanka L, Traneus E, Bassler N. A systematic review on the usage of averaged LET in radiation biology for particle therapy. Radiother Oncol 2021;161:211–21. https://doi.org/10.1016/j.radonc.2021.04.007.
[43] Grzanka L, Ardenfors O, Bassler N. Monte Carlo simulations of spatial LET distributions in clinical proton beams. Radiat Prot Dosim 2018;180:296–9. https://doi.org/10.1093/rpd/ncx272.
[44] Grassberger C, Paganetti H. Elevated LET components in clinical proton beams. Phys Med Biol 2011;56:6677–91. https://doi.org/10.1088/0031-9155/56/20/011.
[45] Mairani A, Dokic I, Magro G, Tessonnier T, Bauer J, Böhlen TT, et al. A phenomenological relative biological effectiveness approach for proton therapy based on an improved description of the mixed radiation field. Phys Med Biol 2017;62:1378–95. https://doi.org/10.1088/1361-6560/aa51f7.
[46] Hahn C, Ödén J, Dasu A, Vestergaard A, Fuglsang Jensen M, Sokol O, et al. Towards harmonizing clinical linear energy transfer (LET) reporting in proton radiotherapy: a European multi-centric study. Acta Oncol 2022;61:206–14. https://doi.org/10.1080/0284186X.2021.1992007.